DMD Fast Forward. Published on March 9, 2018 as DOI: 10.1124/dmd.117.079673
This article has not been copyedited and formatted. The final version may differ from this version.

Pharmacokinetics-Based Identification of Potential Therapeutic Phthalides from XueBiJing, a Chinese Herbal Injection Used in Sepsis Management

Nating Zhang, Chen Cheng, Olajide E Olaleye, Yan Sun, Li Li, Yühong Huang, Feifei Du, Junling Yang, Fengqing Wang, Yanhong Shi, Fang Xu, Yanfen Li, Qi Wen, Naixia Zhang, and Chuan Li

State Key Laboratory of Drug Research, Shanghai Institute of Materia Medica, Chinese Academy of Sciences, Shanghai, China (N-T.Z., C.C., O.E.O, Y.S., L.L., F.D., J.Y., F.W., Y-H.S, F.X., Q.W., N-X.Z., C.L.); University of Chinese Academy of Sciences, Beijing China (N-T.Z., C.L.); Second Affiliated Hospital, Tianjin University of Traditional Chinese Medicine, Tianjin, China (Y.H., Y.L.)

DMD Fast Forward. Published on March 9, 2018 as DOI: 10.1124/dmd.117.079673
This article has not been copyedited and formatted. The final version may differ from this version.

Running Title: Circulating Phthalides from XueBiJing

Address correspondence to:

Professor Chuan Li, Laboratory for DMPK Research of Herbal Medicines, Shanghai Institute of Materia Medica, Chinese Academy of Sciences, 501 Haike Road, Zhangjiang Hi-Tech Park, Shanghai 201203, China. E-mail: chli@simm.ac.cn

Number of Text Pages: 19

Number of Tables: 6

Number of Figures: 7

Number of References: 44

Number of Words in Abstract Section: 250

Number of Words in Introduction Section: 666

Number of Words in Discussion Section: 1225

Abbreviations:

$AUC_{0-\infty}$, area under concentration-time curve from 0 to infinity; C_{max}, maximum plasma concentration; CL_{int}, intrinsic clearance; CL_R, renal clearance; $CL_{tot,p}$, total plasma clearance; $Cum.A_{e\text{-}U\ 0-24h}$, cumulative amount excreted into urine from 0 to 24 h; $Cum.A_{e\text{-}B\ 0-24h}$, cumulative amount excreted into bile from 0 to 24 h; $f_{e\text{-}B}$, fractional biliary excretion; $f_{e\text{-}U}$, fractional urinary excretion; f_u, unbound fraction of compound in plasma; GFR, glomerular filtration rate; HLM, human liver microsomes; K_m, Michaelis constant; nK, total binding constant; P_{app}, apparent permeability coefficient; RLM, rat liver microsomes; TCM, traditional Chinese medicine; UGT, uridine 5′-diphosphoglucuronosyltransferase; V_{max}, maximum velocity; V_{SS}, apparent volume of distribution at steady state.

DMD Fast Forward. Published on March 9, 2018 as DOI: 10.1124/dmd.117.079673
This article has not been copyedited and formatted. The final version may differ from this version.

ABSTRACT

XueBiJing, an injectable five-herb preparation, has been incorporated into routine sepsis care in China. Phthalides, originating from XueBiJing's component herbs *Ligusticum chuanxiong* rhizomes and *Angelica sinensis* roots, are believed to contribute to its therapeutic effects due to their presence in the preparation and antisepsis-related properties. This investigation aimed to identify potential therapeutic phthalides that are bioavailable to act on XueBiJing's therapeutic targets and that could serve as pharmacokinetic markers to supplement classical biomarkers for sepsis care. Among 10 phthalides detected in XueBiJing, senkyunolides I and G were the major circulating phthalides in human subjects, but their different pharmacokinetics might influence their contribution to XueBiJing's therapeutic action. Senkyunolide I exhibited a large distribution volume (1.32 l/kg) and was moderately bound in plasma (54% unbound), whereas senkyunolide G exhibited a small distribution volume (0.10 l/kg) and was extensively bound in plasma (3% unbound). Clearance of senkyunolide I from the systemic circulation was governed by UGT2B15-mediated hepatic glucuronidation; the resulting electrophilic glucuronides were conjugated with GSH in the liver. Senkyunolide G was selectively bound to albumin (99%) in human plasma. To our knowledge, the human pharmacokinetic data of XueBiJing's phthalides are reported here for the first time. Based on this investigation and such investigations for the other component herbs, follow-up pharmacodynamic assessments of bioavailable herbal compounds are planned to understand XueBiJing's chemical basis responsible for its therapeutic action. Senkyunolides I and G, having the preceding disposition characteristics that could be detectably altered by septic pathophysiology, could serve as pharmacokinetic markers for sepsis care.

DMD Fast Forward. Published on March 9, 2018 as DOI: 10.1124/dmd.117.079673
This article has not been copyedited and formatted. The final version may differ from this version.

Introduction

Sepsis is life-threatening organ dysfunction caused by a dysregulated host response to infection (Singer et al., 2016). Current pharmacotherapy of sepsis relies on timely and appropriate antibiotics and resuscitation therapies. Despite progress in understanding the pathophysiology, search for pharmacotherapies for modulating the septic response appears to be unsuccessful (Cohen et al., 2015).

XueBiJing, an intravenous preparation approved by the China Food and Drug Administration (China FDA) in 2004, has been incorporated into routine sepsis care (Chinese Society of Critical Care Medicine, 2015). In China, about 800,000 patients use XueBiJing each year and 80% of them are patients with sepsis or septic shock. XueBiJing is prepared from a combination of *Carthamus tinctorius* flowers (Honghua in Chinese), *Paeonia lactiflora* roots (Chishao), *Ligusticum chuanxiong* rhizomes (Chuanxiong), *Angelica sinensis* roots (Danggui), and *Salvia miltiorrhiza* roots (Danshen). Many clinical studies in China have provided evidence that adding XueBiJing to conventional management of sepsis reduces septic patients' 28-day mortality and incidence of complications, improves their Acute Physiology and Chronic Health Evaluation II scores and prognosis, and shortens their stay in intensive care units, with low incidence of side effects (Chen and Li, 2013; Gao et al., 2015). A recent prospective, multicenter, randomized, single-blinded clinical trial in 710 patients with severe pneumonia showed that adding XueBiJing (100 ml b.i.d for 5–7 days) to treatment could significantly reduce mortality (15.9% and 24.6% for the XueBiJing-treated and control groups, respectively) and increase percentage of patients having improved pneumonia severity index (60.8% and 46.3%, respectively) (Song et al., 2016). XueBiJing was found to inhibit uncontrolled release of inflammatory mediators, relieve an early overabundant innate immune response and

DMD Fast Forward. Published on March 9, 2018 as DOI: 10.1124/dmd.117.079673
This article has not been copyedited and formatted. The final version may differ from this version.

potentially cumulative immunosuppression, attenuate crosstalk between inflammation and coagulation, protect endothelial cells, and maintain physiological functions of vital organs (Yin and Li, 2014; Liu et al., 2015; Dong et al., 2016). Unlike for most investigational antiseptic drugs developed from bench to bedside, research on XueBiJing proceeds from bedside to bench to bedside. Further research on this herbal medicine might facilitate a better understanding of pathophysiology of sepsis and discovery of new antiseptic pharmacotherapies.

Despite the promising results of clinical studies, XueBiJing's chemical basis responsible for its therapeutic action is largely unknown; this impedes exploring how XueBiJing compounds and their synergistic interactions can affect sepsis. Such chemical basis comprises those constituents, of the herbal medicine, having sufficient bioavailability to and biopersistence at the sites of medicine's therapeutic action after dosing and having intrinsic ability to produce desired pharmacodynamic effects in their exposure forms, unchanged and/or metabolized. Here, the bioavailability means the amounts and ability of the medicine's constituents and/or their bioactive metabolites to pass through multiple biological barriers in the body to access the action sites, while the biopersistence means the residence time of these compounds at the action sites for their pharmacodynamic effects to have therapeutically meaningful durations. Hence, multi-compound pharmacokinetic research on XueBiJing has been proposed and the results will prioritize its compounds for pharmacodynamic assessments. Meanwhile, such research could also help identify those herbal compounds with detectably altered pharmacokinetics in response to sepsis as pharmacokinetic markers to reflect and predict abnormal cellular processes in tissues and treatment-caused reversion toward normal states. Based on their antisepsis-related properties and presence in XueBiJing, four types of compounds, i.e.,

Chuanxiong/Danggui phthalides, Honghua flavonoids, Chishao monoterpene glycosides, and Danshen catechols (Huang et al., 2011), are being investigated in our ongoing serial pharmacokinetic research on the medicine (Cheng et al., 2016a; Li et al., 2016). As a part of the research, the current investigation focused on phthalides. Many phthalides, as pure isolates from Chuanxiong and Danggui, have shown antiinflammatory, antioxidant, and neuroprotective properties in cell- and animal-based studies (Qi et al., 2010; Or et al., 2011; Feng et al., 2012). The aim of this investigation was to identify potential therapeutic phthalides that are bioavailable to act on XueBiJing's therapeutic targets and that could serve as pharmacokinetic markers to supplement classical biomarkers for sepsis care. To our knowledge, the human pharmacokinetic data of phthalides in XueBiJing are reported here for the first time.

Materials and Methods

A detailed description of materials and methods is provided in the Supplemental Materials and Methods, which is available online.

Drug Products, Chemicals, and Reagents. Samples of nine lots (1309271, 1309281, 1309291, 1309301, 1405301, 1406161, 1408191, 1410081, and 1501181) of XueBiJing with a China FDA drug ratification number of GuoYaoZhunZi-Z20040033 were obtained from Tianjin Chasesun Pharmaceutical Co., Ltd. (Tianjin, China). Each milliliter of XueBiJing is prepared from a combination of 0.1 g each of Honghua (*C. tinctorius* flowers), Chishao (*P. lactiflora* roots), Chuanxiong (*L. chuanxiong* rhizomes), Danggui (*A. sinensis* roots), and Danshen (*S. miltiorrhiza* roots), yielding an herb-to-injection ratio of 1:2. The final product of XueBiJing is a sterile and nonpyrogenic dosage form for intravenous administration and is standardized to contain 1.0–1.7 mg/ml paeoniflorin and 0.2–0.5 mg/ml hydroxysafflor yellow A.

DMD Fast Forward. Published on March 9, 2018 as DOI: 10.1124/dmd.117.079673
This article has not been copyedited and formatted. The final version may differ from this version.

Crude material samples of Chuanxiong (*L. chuanxiong* rhizomes) and Danggui (*A. sinensis* roots) were also obtained from Tianjin Chasesun Pharmaceuticals.

Senkyunolides A, G, H, I, and N, 3-*n*-butylenephthalide, 3-*n*-butylphthalide, 3-hydroxy-3-*n*-butylphthalide, levistolide A, and *Z*-ligustilide were obtained from Shanghai Yuanye Bio-Technology Co., Ltd. (Shanghai, China) or Shanghai Standard Technology Co., Ltd. (Shanghai, China); the compounds' purity was ≥ 98%. Pooled human liver microsomes (HLM), prepared from Chinese male and female human livers, was obtained from Research Institute for Liver Diseases (Shanghai) Co., Ltd. (Shanghai, China), while pooled rat liver microsomes (RLM) was prepared from livers of male Sprague-Dawley rats in-house by differential centrifugation. cDNA-expressed human uridine 5′-diphosphoglucuronosyltransferase (UGT) enzymes were obtained from Corning Gentest (Woburn, MA). Reduced GSH, UDP-GlcUA, and human plasma γ-globulins were obtained from Sigma-Aldrich (St. Louis, MO). Human plasma albumin, α_1-acid glycoprotein, high density lipoproteins, low density lipoproteins, and very low density lipoproteins were obtained from Athens Research & Technology (Athens, GA). Chemical reagents and organic solvents were obtained from Sinopharm Chemical Reagent Co., Ltd. (Shanghai, China).

Human Pharmacokinetic Study of XueBiJing. A single-center, open-label human study of XueBiJing was performed at the National Clinical Research Center of the Second Affiliated Hospital of Tianjin University of Traditional Chinese Medicine (Tianjin, China). The study procedure was approved by an ethics committee of clinical investigation at the hospital, and had been carried out in accordance with the Declaration of Helsinki. The study was registered in Chinese Clinical Trials Registry (www.chictr.org) with a registration number of ChiCTR-ONRC-13003932. Healthy

volunteers (18–35 years of age) were recruited and gave written informed consent forms to participate in the study.

Human subjects were randomly assigned to three groups (six male and six female in each group). Human subjects received a single dose of one of the following the dosage regimens: (1) a single 1.25-h infusion of 100-ml preparation (diluted with 100 ml of 0.9% NaCl injection), (2) a single 2.5-h infusion of 100-ml preparation (diluted with 200 ml of 0.9% NaCl injection), or (3) a single 1.25-h infusion of 50-ml preparation (diluted with 100 ml of 0.9% NaCl injection). The test dosage regimens were designed according to the label dose of XueBiJing (100 ml/time/person) at infusion rate that is commonly used for XueBiJing in clinics to treat patients with sepsis (regimen 1) and the label doses of XueBiJing (50 and 100 ml/time/person) at infusion rate that is generally recommended for intravenous administration of Chinese herbal injections (regimens 2 and 3). Serial blood and urine samples were collected just before starting the infusion and, at intervals, up till 24 h after starting the infusion (Supplemental Table 1). In addition, the six male subjects of regimen 3 continued to receive the same dose of XueBiJing each day for the following six days, and both blood and urine samples were collected (Supplemental Table 1). All blood samples were heparinized and centrifuged for plasma preparation.

Supportive Rat Pharmacokinetic Studies of XueBiJing. All animal care and experimental procedures complied with the Guide for the Care and Use of Laboratory Animals adopted and promulgated by the U.S. National Institutes of Health and were approved by the Institutional Animal Care and Use Committee at Shanghai Institute of Materia Medica (Shanghai, China). Male Sprague-Dawley rats (230–270 g, 6–8 weeks) were obtained from Sino–British SIPPR/BK Laboratory Animal Co., Ltd (Shanghai, China). Some rats received femoral-artery-cannulation for blood sampling,

DMD Fast Forward. Published on March 9, 2018 as DOI: 10.1124/dmd.117.079673
This article has not been copyedited and formatted. The final version may differ from this version.

and others undergone bile-duct-cannulation for bile sampling (Chen et al., 2013). A total of 62 rats were used in the experiments described here.

In the first study, 18 rats were randomly assigned to three groups (six rats in each group). Rats received a single 0.5-h intravenous infusion of XueBiJing at 10, 30, or 90 ml/kg. The dose 10 ml/kg for rats was derived from the label dose of XueBiJing for patients (100 ml/time/person) according to dose normalization by body surface area (Reagan-Shaw et al., 2008). Serial blood samples were collected just before starting the infusion and, at intervals, up till 24 h after starting the infusion. In the second study, six rats, housed individually in metabolic cages, received a single 0.5-h intravenous infusion of XueBiJing at 10 ml/kg, and urine and fecal samples were collected just before starting the infusion and, at intervals, up till 24 h after starting the infusion. In the third study, six rats received a single 0.5-h intravenous infusion of XueBiJing at 10 ml/kg, and bile samples were collected just before starting the infusion and, at intervals, up till 24 h after starting the infusion. In the fourth study, 20 rats, under isoflurane anesthesia, were killed by bleeding from the abdominal aorta after an intravenous bolus dose of XueBiJing at 10 ml/kg. The lungs, heart, brain, kidneys, and liver were excised and homogenized, and the bloods were also collected. In the fifth study, 12 rats were randomly assigned to two groups to receive a single 0.5-h intravenous infusion of XueBiJing at 10 ml/kg (each milliliter of XueBiJing containing 0.3 μmol of senkyunolide I) or the injectable solution of purified senkyunolide I at 3.0 μmol/kg. Serial blood samples were collected just before starting the infusion and, at intervals, up till 24 h after starting the infusion. All blood samples were heparinized and centrifuged for plasma preparation.

Supportive In Vitro Characterizations of Phthalides.

Metabolism Studies. In vitro metabolism studies were performed to characterize

DMD Fast Forward. Published on March 9, 2018 as DOI: 10.1124/dmd.117.079673
This article has not been copyedited and formatted. The final version may differ from this version.

tentative XueBiJing phthalide metabolites that had been detected in vivo. Because of detection of glucuronides of XueBiJing phthalides in excretory samples of human subjects and rats receiving XueBiJing, senkyunolides I, G, H and N, and 3-hydroxy-3-*n*-butylphthalide were incubated with UDP-GlcUA-fortified HLM or UDP-GlcUA-fortified RLM to glucuronidate these phthalides, and the incubation conditions were as described by Hu et al. (2013). Such in vitro glucuronidation of senkyunolide I was repeated, but with addition of GSH into the incubation. In addition, senkyunolide I was incubated directly with GSH. The cDNA-expressed human UGTs were used to identify which human UGT isoforms could mediate glucuronidation of senkyunolide I. UGT1A9, UGT2B15, UGT2B17, HLM, and RLM were compared with respect to their metabolic capability for mediating glucuronidation of senkyunolide I.

Assessment of Protein Binding (Total Plasma and Individual Proteins). Unbound fraction in plasma (f_u) was assessed for senkyunolides I, G, H, and N, and 3-hydroxy-3-*n*-butylphthalide by a method of rapid ultrafiltration (at 13,362 *g* and 37 ℃ for 3 min) by Guo et al. (2006). This method was also used in identification of proteins responsible for the binding of senkyunolides I and G in human plasma by individually spiking the test compounds into solutions of isolated test proteins at their physiological concentrations (Urien et al., 1992).

Caco-2 Cell-based Assessment of Membrane Permeation Rate. To help understand their in vivo reach, rates of membrane permeation of senkyunolides I, G, H, and N, and 3-hydroxy-3-*n*-butylphthalide were assessed using Caco-2 cell monolayers under “sink” conditions (Dai et al., 2008).

Assessment of Blood-plasma Partition. Blood-to-plasma concentration ratios were determined for senkyunolides I and G in human and for senkyunolides I, G, H,

DMD Fast Forward. Published on March 9, 2018 as DOI: 10.1124/dmd.117.079673
This article has not been copyedited and formatted. The final version may differ from this version.

and N, and 3-hydroxy-3-*n*-butylphthalide in rats using a method by Chen et al. (2013).

Preparation of Glucuronides of Senkyunolide I and Their Structural Elucidation by NMR. The glucuronides of senkyunolide I were biosynthesized by incubating isolated senkyunolide I with UDP-GlcUA-fortified RLM and purified by liquid chromatography. The purified compounds were analyzed by NMR spectrometry using a Bruker AVANCE III-500 MHz spectrometer (Bremen, Germany) to elucidate their structures.

Detection and Characterization of Unchanged and Metabolized Phthalides. A Waters Synapt G2 high definition time-of-flight mass spectrometer (Manchester, UK), interfaced via a Zspray/LockSpray electrospray ionization source with a Waters Acquity UPLC separation module (Milford, MA), was used to analyze phthalides in samples of XueBiJing, pulverized Chuanxiong, and pulverized Danggui and to analyze unchanged and metabolized phthalides in samples obtained from human, rat, and in vitro studies. To facilitate these analyses, pre-analysis literature mining was conducted on phthalides of Chuanxiong and/or Danggui origin with respect to their names, chemical structures, presence in raw materials of Chuanxiong and Danggui and in Chinese medicines containing these herbs, pharmaceutical processing-related chemotransformation, liquid chromatography/mass spectrometry-based analysis, pharmacokinetics and metabolism, antisepsis-related properties, and toxicities. In addition, detection of metabolized phthalides in samples from human and rat studies was also facilitated by Accelrys metabolite database (version 2015.1; San Diego, CA), which was used to predict possible metabolic pathways of phthalides (Williams et al., 2012).

Quantification of Phthalides. An AB Sciex API 4000 Q Trap mass spectrometer (Toronto, Canada), interfaced via a Turbo V ion source with a Waters

DMD Fast Forward. Published on March 9, 2018 as DOI: 10.1124/dmd.117.079673
This article has not been copyedited and formatted. The final version may differ from this version.

Acquity UPLC separation module, was used to quantify phthalides and related compounds in samples of different types. Matrix-matched calibration curves of senkyunolides I, H, G, and N, 3-hydroxy-3-n-butylphthalide, and senkyunolide I-7-*O*-β-glucuronide were constructed using weighted ($1/X$ or $1/X^2$) linear regression of the peak areas (Y) of the analytes against the corresponding nominal analytes' concentrations (X; 6, 19, 56, 167, 500, 1500, and 4500 nM), and the curves showed good linearity ($r^2 > 0.99$). Sample preparation was performed using methanol-based treatment at a volumetric methanol-to-sample ratio of 3:1 for samples of human and rat studies and at a ratio of 1:1 for samples of in vitro metabolism studies. The quantification method was validated according to the European Medicines Agency Guideline on Bioanalytical Method Validation (2012) to demonstrate their reliability and reproducibility for the intended use. The assays' lower limits of quantification were 19–56 nM for the analytes and the upper limits of quantification were 4500 nM. The intra-batch accuracy and precision were 86–112% and 2–15%, respectively, while the inter-batch values were 95–113% and 3–12%, respectively. The coefficients of variation of matrix factors were 1.3–13.6%, which were within the required range, i.e., ≤ 15%. The stability of analytes under conditions mimicking the analytical process was evaluated: after storage at 24 ℃ for 5 h, after storage at 8 ℃ for 24 h, and after three freeze-and-thaw cycles. The test compounds were stable under the test conditions, because the results, i.e., −15–9%, met the acceptance criterion (the measured mean concentration being within ±15% of the nominal concentration).

Data Analysis. Pharmacokinetic parameters were estimated by a noncompartmental method using Thermo Scientific Kinetica 5.0 software package (version 5.0; Philadelphia, PA). Michaelis constant (K_m) and maximum velocity (V_{max}) were estimated using GraphPad Prism software (version 5.01; San Diego, CA). Dose

DMD Fast Forward. Published on March 9, 2018 as DOI: 10.1124/dmd.117.079673
This article has not been copyedited and formatted. The final version may differ from this version.

proportionality of senkyunolide I in the rats was assessed using the regression of log-transformed data (the Power model), with the criteria calculated according to a method by Smith et al. (2000). Statistical analysis was performed using IBM SPSS Statistics software (version 19.0; Somers, NY). All data are expressed as the mean ± S.D. $P < 0.05$ was considered the minimum level of statistical significance.

Results

Phthalides Detected in XueBiJing and Their Relative Abundance. As the first step in pharmacokinetic investigation of phthalides after dosing XueBiJing, analysis of the chemical composition of phthalides in the medicine was performed to understand which and how much phthalides were introduced into the bloodstream by dosing the medicine. A total of 10 phthalides (Log*P*, 0.8–3.0) were detected in XueBiJing (Table 1 and Fig. 1). More lipophilic phthalides (Log*P*, 3.0–5.0), including *Z*-ligustilide (**5**) [the most abundant phthalide in the raw herb materials Chuanxiong (*L. chuanxiong* rhizomes) and Danggui (*A. sinensis* roots)], were not detected in the preparation.

The detected phthalides were ranked according to their dose levels from XueBiJing at a label dose of 100 ml. After ranking, the detected phthalides were graded as Level I (10–100 μmol/day), comprising senkyunolide I (**15**) (29.3 μmol/day); Level II (1–10 μmol/day), comprising senkyunolides H (**16**), G (**12**), and N (**17**), 3-hydroxy-3-*n*-butylphthalide (**10**), *Z*-6,7-epoxyligustilide (**9**), and 6,7-dihydroxyligustilide (**14**) (1.1–6.5 μmol/day); and Level III (< 1 μmol/day), comprising the remaining phthalides (0.2–0.5 μmol/day). The dose of the Level I phthalide, the sum of the doses of the Level II phthalides, and the sum of the doses of the Level III phthalides accounted for 56.9%, 41.0%, and 2.0% of the total dose of the phthalides in the preparation, respectively. XueBiJing exhibited lot-to-lot variability

DMD Fast Forward. Published on March 9, 2018 as DOI: 10.1124/dmd.117.079673
This article has not been copyedited and formatted. The final version may differ from this version.

of 9.6% for the Level I phthalide **15**, 4.0–12.7% for Level II phthalides, and 12.6–54.0% for Level III phthalides (Table 1). These data suggested that XueBiJing exhibited good quality consistency, with respect to individual doses of its major phthalides.

Systemic Exposure to Phthalides in Human Subjects and Rats after Dosing XueBiJing. In human subjects, five unchanged phthalides were detected in plasma after starting an intravenous infusion of XueBiJing; they were not detected before dosing (Fig. 2 and Supplemental Table 2). Senkyunolides I (**15**) and G (**12**) exhibited notably higher levels of systemic exposure than the other detected phthalides senkyunolide H (**16**), senkyunolide N (**17**), and 3-hydroxy-3-*n*-butylphthalide (**10**). These circulating phthalides, except **12**, were also detected in urine, after dosing, with fractions of dose excreted ($f_{e\text{-}U}$) of 3.0–18.3%. Chemical structures of these circulating phthalides are also shown in Fig. 2.

In rats, senkyunolides I (**15**), H (**16**), G (**12**), and N (**17**), and 3-hydroxy-3-*n*-butylphthalide (**10**) were detected in plasma after dosing XueBiJing (Fig. 2 and Supplemental Table 2). However, unlike in human subjects, **12** exhibited a significantly lower exposure level in rats, relative to **15**. These circulating phthalides were also detected in urine, except **12**, and in bile, except **12** and **10** (Fig. 2). Their $f_{e\text{-}U}$ and fractions of dose excreted into bile ($f_{e\text{-}B}$) were 0.6–2.8% and 0.2–3.7%, respectively. Trace amounts of these phthalides were detected in rat feces.

The preceding excretory data suggested that the circulating phthalides were cleared mainly via metabolism. However, no circulating metabolites of phthalides were detected in human subjects or rats after dosing XueBiJing. Several metabolites of senkyunolides I (**15**) and G (**12**) were detected in excretory samples (Supplemental Tables 3 and 4), but metabolites of the other circulating phthalides were negligible or

DMD Fast Forward. Published on March 9, 2018 as DOI: 10.1124/dmd.117.079673
This article has not been copyedited and formatted. The final version may differ from this version.

not detected. For **15**, its glucuronides (**M15$_{G-1}$** and **M15$_{G-2}$**), dehydrated glutathione conjugates (**M15$_{GSH-1}$** and **M15$_{GSH-2}$**), and degradation products of the glutathione conjugates (the cysteinylglycine conjugates **M15$_{Cys-Gly-1}$** and **M15$_{Cys-Gly-2}$** and the cysteine conjugates **M15$_{Cys-1}$** and **M15$_{Cys-2}$**) were detected in rat bile. **M15$_{G-1}$**, **M15$_{G-2}$**, and *N*-acetylcysteine conjugates (**M15$_{NAC-1}$** and **M15$_{NAC-2}$**) were detected in rat urine. **M15$_{G-1}$**, **M15$_{G-2}$**, **M15$_{Cys-1}$**, and **M15$_{Cys-2}$** were detected in human urine. For **12**, its glucuronide (**M12$_{G}$**) was detected in rat bile and urine, but not in human urine.

In Vitro Metabolism of Phthalides. Additional in vitro metabolism studies were performed to better understand in vivo elimination of the circulating XueBiJing phthalides, and the results are shown in Table 2 and Fig. 3–5. Incubation of senkyunolide I with UDP-GlcUA-fortified HLM led to the formation of the glucuronides **M15$_{G-1}$** and **M15$_{G-2}$**, with an **M15$_{G-2}$**-to-**M15$_{G-1}$** peak area ratio of 66; such a ratio for RLM was 5. **M15$_{G-1}$** and **M15$_{G-2}$** were characterized as senkyunolide I-6-*O*-β-glucuronide and senkyunolide I-7-*O*-β-glucuronide, respectively, using NMR data (Supplemental Table 5). Notably, senkyunolide I was found to be primarily glucuronized by human UGT2B15, with UGT1A9 and UGT2B17 playing a minor role (Fig. 3). Glucuronidation of senkyunolide I into senkyunolide I-7-*O*-β-glucuronide was saturable, with K_m, V_{max}, and CL_{int} of 18.4 ± 1.0 μM, 291 ± 5 pmol/min/mg protein, and 15.8 μl/min/mg protein, respectively, for cDNA-expressed human UGT2B15; 34.7 ± 3.2 μM, 7360 ± 254 pmol/min/mg protein, and 212 μl/min/mg protein, respectively, for HLM; and 185 ± 5 μM, 12305 ± 122 pmol/min/mg protein, and 66.5 μl/min/mg protein, respectively, for RLM. Another important finding was the electrophilicity of the glucuronides of senkyunolide I. As shown in Fig. 4, dehydrated GSH conjugates of senkyunolide I (**M15$_{GSH-1}$** and **M15$_{GSH-2}$**) were formed by GSH replacement of glucuronic acid in a second

DMD Fast Forward. Published on March 9, 2018 as DOI: 10.1124/dmd.117.079673
This article has not been copyedited and formatted. The final version may differ from this version.

metabolic reaction. No GSH conjugate was detected after incubation of senkyunolide I directly with GSH. Both the in vivo metabolite profiling and the in vitro metabolism study suggested that the glucuronidation governed clearance of senkyunolide I (**15**) from the systemic circulation.

Glucuronidation of senkyunolide G occurred by incubation of this phthalide with UDP-GlcUA-fortified RLM and UDP-GlcUA-fortified HLM, but the formation rate of the glucuronide (**M12G**) was quite slow in the latter. Glucuronides of senkyunolide H, senkyunolide N, and 3-hydroxy-3-*n*-butylphthalide were also formed in vitro with UDP-GlcUA-fortified HLM and UDP-GlcUA-fortified RLM, but were negligibly detected in vivo. Figure 5 shows the proposed metabolic pathways of senkyunolides I (**15**) and G (**12**).

Pharmacokinetic Characteristics of Circulating XueBiJing Phthalides in Human Subjects and Rats. Figure 6 depicts the plasma concentration-time profiles of senkyunolides I (**15**) and G (**12**) in human subjects who intravenously received XueBiJing; Table 3 summarizes their pharmacokinetic data. The circulating **15** and **12** exhibited dose- and injection-rate-dependent maximum plasma concentration (C_{max}) and dose-dependent area under concentration-time curve from 0 to infinity ($AUC_{0-\infty}$). Neither C_{max} nor $AUC_{0-\infty}$ of **15** and **12** exhibited significant gender differences (P = 0.17–0.99), after correcting the compound doses for the subject's body weight. The apparent volume of distribution at steady state (V_{SS}) and total plasma clearance ($CL_{tot,p}$) also showed no significant gender differences (P = 0.13–0.98). The mean V_{SS} of **15** for all the groups of dosage regimen was 13.2 times as much as that of **12** (P = 2.7×10^{-11}), while the mean $CL_{tot,p}$ of **15** was 26.5 times as much as that of **12** (P = 5.2×10^{-11}). The mean terminal $t_{1/2}$ of **12** was 2.7 times as much as that of **15** (P = 3.7×10^{-23}). Apart from the glomerular filtration, tubular reabsorption was probably also

DMD Fast Forward. Published on March 9, 2018 as DOI: 10.1124/dmd.117.079673
This article has not been copyedited and formatted. The final version may differ from this version.

involved in renal excretion of **15**, as indicated by its mean $CL_R/(GFR \times f_u)$ ratio (Table 3). Such tubular reabsorption might be a reason for non-detection of **12** in urine. During subchronic daily intravenous infusions of XueBiJing for seven consecutive days, accumulation of circulating **15** and **12** appeared to be negligible (Fig. 6 and Supplemental Table 6).

Rat studies were designed to obtain some additional pharmacokinetic information that, due to ethical reason, was not obtainable via the human study but that is important to better understand the pharmacokinetics and disposition of XueBiJing compounds. Similarities and differences between humans and rats in pharmacokinetics of XueBiJing phthalides were considered (Supplemental Table 7), and further rat studies focused on senkyunolide I (**15**) due to the interspecies similarity. As a result, rat systemic exposure to **15** (C_{max} and $AUC_{0-\infty}$) increased proportionally as the dose of XueBiJing increased from 10 ml/kg to 90 ml/kg, while the V_{SS}, $CL_{tot,p}$, and $t_{1/2}$ remained basically constant (Table 4 and Fig. 7). Effects of the matrix components of the preparation on the pharmacokinetics of **15** was assessed in rats by comparing the pharmacokinetic parameters obtained for the compound after dosing XueBiJing with those after dosing an injectable solution of purified senkyunolide I. Other compounds in XueBiJing exhibited limited influence on the pharmacokinetics of **15** (Supplemental Table 8 and Fig. 7). Consistent with its large V_{SS} in rats, **15** distributed extensively into rat lungs, heart, brain, kidneys, and liver (Fig. 7).

Table 5 summarizes pharmacokinetic data related to in vivo reach of circulating XueBiJing phthalides. Senkyunolides I (**15**), G (**12**), H (**16**), and N (**17**), and 3-hydroxy-3-*n*-butylphthalide (**10**) exhibited good membrane permeability, as indicated by their Caco-2-based apparent permeability coefficients (P_{app}). However,

DMD Fast Forward. Published on March 9, 2018 as DOI: 10.1124/dmd.117.079673
This article has not been copyedited and formatted. The final version may differ from this version.

their extents of binding in human plasma were quite different, as indicated by their f_u. Notably, senkyunolide G was selectively bound to albumin, rather than to other human plasma proteins, i.e., α_1-acid glycoprotein, γ-globulins, high density lipoproteins, low density lipoproteins, and very low density lipoproteins, as indicated by the proteins' relative binding capabilities (Table 6).

Discussion

In China, herbal medicines are extensively used in clinics and prescribed by both Western medicine physicians and traditional Chinese medicine (TCM) physicians. Ambitious attempt has been made to develop Chinese herbal medicines in line with modern standards, and the annual GDP of Chinese TCM pharmaceutical industry has increased from 23 billion RMB (about US$ 3.5 billion) in 1996 to 786 billion RMB (US$ 121 billion) in 2015 (Zhang and Chen, 2016). Currently, the China FDA requires herbal medicines, before marketing, to be proved safe and effective. However, earlier-approved Chinese herbal medicines, having therapeutic claims largely based on their established use in TCM, generally have not been extensively tested, owing to the science and technology available at the time. Recently, a number of patent herbal medicines, manufactured by major Chinese TCM pharmaceutical companies, have shown therapeutic benefits in rigorous clinical studies similar to those for contemporary pharmaceuticals (Wang et al., 2011; Li et al., 2013; Shang et al., 2013; Zhang et al., 2014). Because of the complex chemical composition of such medicines, adequate assessment of their efficacy and safety needs not only clinical studies but identification of the medicines' chemical basis responsible for their therapeutic actions as well. Hence, pharmacokinetic research on Chinese herbal medicines, particularly those with proved efficacy and safety, has been proposed to serve as a crucial step in identifying such chemical basis (Lu et al., 2008; Liu et al., 2009; Hu et

al., 2013; Cheng et al., 2016b). This pharmacokinetics-guided strategy is new and could be more successful than the classical phytochemistry-initiated strategy.

As a part of our ongoing serial pharmacokinetic research on XueBiJing, this investigation focused on phthalides, originating from the component herbs Chuanxiong and Danggui, and was performed in two steps, i.e., 1) identifying major circulating phthalides after dosing XueBiJing and 2) investigating pharmacokinetic factors that are important for their pharmacodynamic effects, mainly their in vivo reach, and the factors governing their systemic exposure. As a result, unchanged senkyunolides I (**15**) and G (**12**) were identified, in human subjects, as the major circulating phthalides out of the 10 phthalides detected in the dosed XueBiJing. However, **15** and **12** exhibit different pharmacokinetic characteristics. Although both the phthalides had good membrane permeability, their binding in human plasma was quite different. This difference, together with the significant differences in V_{SS}, suggested that these two phthalides could differ in their in vivo reach. After dosing XueBiJing, **15** was extensively distributed and could well reach both extracellular and intracellular receptors. Among the major circulating herbal compounds identified in our pharmacokinetic research on XueBiJing, **15** was the only XueBiJing compound well detected in rat brain, suggesting its good brain penetration. This finding may be important, because XueBiJing is used in treatment of patients with sepsis showing brain dysfunction. In contrast, **12** resided largely in plasma; this probably limited its bioavailability to act on therapeutic targets. Meanwhile, **15** and **12** also substantially differed in $CL_{tot,p}$. Clearance of **15** from the systemic circulation was rapid and governed mainly by glucuronidation. Clearance of **12** from the systemic circulation was quite slow, probably due to very slow glucuronidation in humans. Significantly smaller V_{SS} and lower $CL_{tot,p}$ of **12**, relative to **15**, resulted in its higher levels of

systemic exposure in humans, even though its dose from XueBiJing was only 15% of that of **15**. It is worth mentioning that the high exposure level of **12** represented its total (bound and unbound) concentration, predominantly comprising the bound concentration rather than the bioavailable unbound concentration.

Sepsis is a complex, heterogeneous, and rapidly evolving life-threatening syndrome; diagnostic and prognostic biomarkers have been used to assist clinicians in treatment decisions (Sandquist and Wong, 2014; Jensen and Bouadma, 2016). However, due to their considerable delay and insufficient specificity and sensitivity for routine employment in clinical practice, classical biomarkers for sepsis care need to be supplemented with new markers. Pharmacokinetic research on an herbal medicine can help identify pharmacokinetic markers originating from the medicine. One type of such markers can reflect the body exposure to the herbal compounds responsible for or related to the medicine's therapeutic action and the associated influencing factors (Lu et al., 2008; Hu et al., 2013; Li, 2017) (Supplemental Table 9). Proposed here is another type of pharmacokinetic markers that can reflect and predict abnormal cellular processes in tissues and treatment-caused reversion toward normal states; these herbal compounds should exhibit pharmacokinetics and disposition that could be detectably altered in response to the disease. In this investigation, hepatic glucuronidation of senkyunolide I (**15**) was found to be mediated primarily by UGT2B15; the resulting glucuronides (**M15$_{G-1}$** and **M15$_{G-2}$**) were electrophilic and conjugated with GSH. Senkyunolide G (**12**) was found to be selectively and extensively bound to albumin in human plasma. Sepsis is accompanied by profound changes in patients, including hepatic, renal, and circulatory dysfunctions; impaired hepatic synthesis of GSH; and altered albumin concentration and structure (Gatta et al., 2012; Bosmann and Ward, 2013; Blot et al., 2014). In addition, growing evidence

DMD Fast Forward. Published on March 9, 2018 as DOI: 10.1124/dmd.117.079673
This article has not been copyedited and formatted. The final version may differ from this version.

has shown that inflammation and immune responses may result in downregulation of drug metabolizing enzymes and transporters (Congiu et al., 2002; Aitken et al., 2006; Harvey and Morgan, 2014). Accordingly, potential exists for septic-pathophysiology-induced alterations in pharmacokinetics and disposition of **15** and **12** and for reversion to a normal xenobiotic disposition state when sepsis burden is substantially reduced in patients across the time course of treatment. Our pilot analysis of XueBiJing compounds in plasma samples of patients with sepsis indicated that unchanged **15** (exhibiting increased systemic exposure in patients, relative to healthy human subjects), **M15$_{G-2}$** (being detectable in patients, but not in healthy human subjects), and **12** (exhibiting increased f_u in patients, relative to healthy human subjects) could serve as pharmacokinetic markers reflecting patients' downregulated UGT2B15, impaired hepatic synthesis of GSH, and decreased plasma albumin, respectively (data not shown).

Similar to synthetic drug discovery and development, the driving motivation for and primary goal of scientific research on Chinese herbal medicines, including pharmacokinetic investigation, is to enrich therapeutic armamentarium, especially for multifactorial diseases. XueBiJing, as an add-on therapy, is promising in modulating the septic response, as shown by many clinical and experimental studies. In summary, among multiple phthalides in XueBiJing, unchanged senkyunolides I (**15**) and G (**12**) are the major circulating phthalides but their different pharmacokinetics in humans might influence their contribution to the medicine's therapeutic action. Based on this pharmacokinetic investigation and such investigations for XueBiJing's other component herbs, follow-up pharmacodynamic assessments of various XueBiJing compounds, unchanged and metabolized, are planned, with respect to antisepsis-related antiinflammatory, immunomodulatory, anticoagulant, and

DMD Fast Forward. Published on March 9, 2018 as DOI: 10.1124/dmd.117.079673
This article has not been copyedited and formatted. The final version may differ from this version.

endothelium-protective activities. UGT2B15-mediated hepatic glucuronidation of **15** is the elimination route governing its clearance from the systemic circulation and the resulting electrophilic glucuronides are conjugated with GSH in the liver, while **12** is selectively and extensively bound to albumin in human plasma. These disposition characteristics of the phthalides could be altered by septic pathophysiology. Additional study in patients with sepsis is planned for XueBiJing to investigate influences of sepsis on pharmacokinetics of bioactive herbal compounds and to identify pharmacokinetic markers to supplement classical biomarkers for sepsis care. Interestingly, senkyunolide I was identified, to our knowledge, as the most selective substrate ever reported for human UGT2B15 (Court et al., 2002; Rowland et al., 2013), while senkyunolide G was found to be selectively bound to human plasma albumin. These naturally occurring phthalides could be useful tool compounds in drug metabolism and pharmacokinetic studies and clinical studies.

DMD Fast Forward. Published on March 9, 2018 as DOI: 10.1124/dmd.117.079673
This article has not been copyedited and formatted. The final version may differ from this version.

Authorship Contributions

Participated in research design: C. Li and N.T. Zhang.

Conducted experiments: N.T. Zhang, Cheng, Olaleye, Sun, L. Li, Huang, Du, Yang, Wang, Shi, Xu, Y. Li, Wen, and N.X. Zhang.

Performed data analysis: C. Li and N.T. Zhang.

Wrote or contributed to the writing of the manuscript: C. Li, N.T. Zhang, and Olaleye.

DMD Fast Forward. Published on March 9, 2018 as DOI: 10.1124/dmd.117.079673
This article has not been copyedited and formatted. The final version may differ from this version.

References

Aitken AE, Richardson TA, and Morgan ET (2006) Regulation of drug-metabolizing enzymes and transporters in inflammation. *Annu Rev Pharmacol Toxicol* **46:** 123–149.

Blot SI, Pea F, and Lipman J (2014) The effect of pathophysiology on pharmacokinetics in the critically ill patient—concepts appraised by the example of antimicrobial agents. *Adv Drug Deliv Rev* **77:** 3–11.

Bosmann M and Ward PA (2013) The inflammatory response in sepsis. *Trends Immunol* **34:** 129–136.

Chen F, Li L, Xu F, Sun Y, Du F-F, Ma X-T, Zhong C-C, Li X-X, Wang F-Q, Zhang N-T, and Li C (2013) Systemic and cerebral exposure to and pharmacokinetics of flavonols and terpene lactones after dosing standardized *Ginkgo biloba* leaf extracts to rats via different routes of administration. *Br J Pharmacol* **170:** 440–457.

Chen Y and Li C-S (2013) The effectiveness of XueBiJing injection in therapy of sepsis: a multicenter clinical study. *Chin J Emerg Med* **22:** 130–135.

Cheng C, Lin J-Z, Li L, Yang J-L, Jia W-W, Huang Y-H, Du F-F, Wang F-Q, Li M-J, Li Y-F, Xu F, Zhang N-T, Olaleye OE, Sun Y, Li J, Sun C-H, Zhang G-P, and Li C (2016a) Pharmacokinetics and disposition of monoterpene glycosides, derived from *Paeonia lactiflora* roots (Chishao), after intravenous dosing of antiseptic XueBiJing injection in human subjects and rats. *Acta Pharmacol Sin* **37:** 530–544.

Cheng C, Du F-F, Yu K, Xu F, Wang F-Q, Li L, Olaleye OE, Yang J-L, Chen F, Zhong C-C, Liu Q-W, Li J, Wang Z-Z, Li C, and Xiao W (2016b) Pharmacokinetics and disposition of circulating iridoids and organic acids in rats intravenously receiving ReDuNing injection. *Drug Metab Dispos* **44:** 1853–1858.

Chinese Society of Critical Care Medicine (2015) Chinese guidelines for management of severe sepsis and septic shock 2014. *Chin Crit Care Med* **27:** 401–426.

Cohen J, Vincent J-L, Adhikari NKJ, Machado FR, Angus DC, Calandra T, Jaton K, Giulieri S, Delaloye J, Opal S, Tracey K, von der Poll T, and Pelfrene E (2015) Sepsis: a roadmap for future research. *Lancet Infect Dis* **15**: 581–614.

Congiu M, Mashford ML, Slavin JL, and Desmond PV (2002) UDP glucuronosyltransferase mRNA levels in human liver disease. *Drug Metab Dispos* **30:** 129–134.

Court MH, Duan S-X, Guillemette C, Journault K, Krishnaswamy S, von Moltke LL, and Greenblatt

DJ (2002) Stereoselective conjugation of oxazepam by human UDP-glucuronosyltransferases (UGTs): *S*-oxazepam is glucuronidated by UGT2B15, while *R*-oxazepam is glucuronidated by UGT2B7 and UGT1A9. *Drug Metab Dispos* **30:** 1257–1265.

Dai J-Y, Yang J-L, and Li C (2008) Transport and metabolism of flavonoids from Chinese herbal remedy Xiaochaihu-tang across human intestinal Caco-2 cell monolayers. *Acta Pharmacol Sin* **29:** 1086–1093.

Davies B and Morris T (1993) Physiological parameters in laboratory animals and humans. *Pharm Res* **10:** 1093–1095.

Dong T-H, Zhang G-P, Dong K, Liu S, and Yao Y-M (2016) Research progress of mechanism of action of XueBiJing injection in the treatment of sepsis. *Chin J Tradit Chin Med West Med Crit Care* **23:** 554–557.

Feng Z-B, Lu Y-P, Wu X-M, Zhao P, Li J-J, Peng B, Qian Z-M, and Zhu L (2012) Ligustilide alleviates brain damage and improves cognitive function in rats of chronic cerebral hypoperfusion. *J Ethnopharmacol* **144:** 313–321.

Gao J, Kong L-B, Liu S, Feng Z-Q, Shen H, and Liu Q-Q (2015) A prospective multicenter clinical study of XueBiJing injection in the treatment of sepsis and multiple organ dysfunction syndrome. *Chin Crit Care Med* **27:** 465–470.

Gatta A, Verardo A, and Bolognesi M (2012) Hypoalbuminemia. *Intern Emerg Med* **7:** S193–S199.

Guo B, Li C, Wang G-J, and Chen L-S (2006) Rapid and direct measurement of free concentrations of highly protein-bound fluoxetine and its metabolite norfluoxetine in plasma. *Rapid Commun Mass Spectrom* **20:** 39–47.

Harvey RD and Morgan ET (2014) Cancer, inflammation, and therapy: effects on cytochrome P450-mediated drug metabolism and implications for novel immunotherapeutic agents. *Clin Pharmacol Ther* **96:** 449–457.

Hu Z-Y, Yang J-L, Cheng C, Huang Y-H, Du F-F, Wang F-Q, Niu W, Xu F, Jiang R-R, Gao X-M, and Li C (2013) Combinatorial metabolism notably affects human systemic exposure to ginsenosides from orally administered extract of *Panax notoginseng* roots (Sanqi). *Drug Metab Dispos* **41:** 1457–1469.

Huang H, Ji L-X, Song S-Y, Wang J, Wei N, Jiang M, Bai G, and Luo G-A (2011) Identification of the major constituents in XueBiJing injection by HPLC-ESI-MS. *Phytochem Anal* **22:** 330–338.

Jensen J-U and Bouadma L (2016) Why biomarkers failed in sepsis. *Intensive Care Med* **42:** 2049–2051.

Li C (2017) Multi-compound pharmacokinetic research on Chinese herbal medicines: approach and methodology. *China J Chin Materia Medica* **42:** 607–617.

Li L, Zhao Y-S, Du F-F, Yang J-L, Xu F, Niu W, Ren Y-H, and Li C (2012) Intestinal absorption and presystemic elimination of various chemical constituents present in GBE50 extract, a standardized extract of *Ginkgo biloba* leaves. *Curr Drug Metab* **13:** 494–509.

Li X-L, Zhang J, Huang J, Ma A-Q, Yang J-F, Li W-M, Wu Z-G, Yao C, Zhang Y-H, Yao W-M, Zhang B-L, and Gao R-L (2013) A multicenter, randomized, double-blind, parallel-group, placebo-controlled study of the effects of Qili Qiangxin capsules in patients with chronic heart failure. *J Am Coll Cardiol* **62:** 1065–1072.

Li X-X, Cheng C, Wang F-Q, Huang Y-H, Jia W-W, Olaleye OE, Li M-J. Li Y-F, and Li C (2016) Pharmacokinetics of catechols in human subjects intravenously receiving XueBiJing injection, an emerging antiseptic herbal medicine. *Drug Metab Pharmacokinet* **31:** 95–98.

Liu H-F, Yang J-L, Du F-F, Gao X-M, Ma X-T, Huang Y- H, Xu F, Niu W, Wang F-Q, Mao Y, Sun Y, Lu T, Liu C-X, Zhang B-L, and Li C (2009) Absorption and disposition of ginsenosides after oral administration of *Panax notoginseng* extract to rats. *Drug Metab Dispos* **37:** 2290–2298.

Liu Y-C, Yao F-H, Chai Y-F, Dong N, Sheng Z-Y, and Yao Y-M (2015) XueBiJing injection promotes M2 polarization of macrophages and improves survival rate in septic mice. *Evid Based Complement Alternat Med* **2015:** 352642.

Lu T, Yang J-L, Gao X-M, Chen P, Du F-F, Sun Y, Wang F-Q, Xu F, Shang H-C, Huang Y-H, Wang Y, Wan R-Z, Liu C-X, Zhang B-L, and Li C (2008) Plasma and urinary tanshinol from *Salvia miltiorrhiza* (Danshen) can be used as pharmacokinetic markers for cardiotonic pills, a cardiovascular herbal medicine. *Drug Metab Dispos* **36:** 1578–1586.

Or TCT, Yang CLH, Law AHY, Li JCB, and Lau ASY (2011) Isolation and identification of anti-inflammatory constituents from *Ligusticum chuanxiong* and their underlying mechanisms of action on microglia. *Neuropharmacology* **60:** 823–831.

Qi H-Y, Siu S-O, Chen Y, Han Y-F, Chu IK, Tong Y, Lau ASY, and Rong J-H (2010) Senkyunolides reduce hydrogen peroxide-induced oxidative damage in human liver HepG2 cells via induction of heme oxygenase-1. *Chem Biol Interact* **183:** 380–389.

Reagan-Shaw S, Nihal M, and Ahmad N (2008) Dose translation from animal to human studies revisited. *Faseb J* **22:** 659–661.

Rowland A, Miners JO, and Mackenzie PI (2013) The UDP-glucuronosyltransferases: their role in drug metabolism and detoxification. *Int J Biochem Cell Biol* **45:** 1121–1132.

Sandquist M and Wong HR (2014) Biomarkers of sepsis and their potential value in diagnosis, prognosis and treatment. *Expert Rev Clin Immunol* **10:** 1349–1356.

Shang H-C, Zhang J-H, Yao C, Liu B-Y, Gao X-M, Ren M, Cao H-B, Dai G-H, Weng W-L, Zhu S-N, Wang H, Xu H-J, and Zhang B-L (2013) Qi-Shen-Yi-Qi dripping pills for the secondary prevention of myocardial infarction: a randomised clinical trial. *Evid Based Complement Alternat Med* **2013:** 738391.

Singer M, Deutschman CS, Seymour CW, Shankar-Hari M, Annane D, Bauer M, Bellomo R, Bernard GR, Chiche J-D, Coopersmith CM, Hotchkiss RS, Levy MM, Marshall JC, Martin GS, Opal SM, Rubenfeld GD, van der Poll T, Vincent J-L, and Angus DC (2016) The third international consensus definitions for sepsis and septic shock (sepsis-3). *J Am Med Assoc* **315:** 801–810.

Smith BP, Vandenhende FR, DeSante KA, Farid NA, Welch PA, Callaghan JT, and Forgue ST (2000) Confidence interval criteria for assessment of dose proportionality. *Pharm Res* **17:** 1278–1283.

Song Y-L, Yao C, Shang H-C, Yao X-Q, and Bai C-X (2016) Late-breaking abstract: intravenous infusion of Chinese medicine XueBiJing significantly improved clinical outcome in severe pneumonia patients in a multiple center randomized controlled clinical trials. *Eur Respir J* **48:** OA3323.

Urien S, Claudepierre P, Meyer J, Brandt R, and Tillement J-P (1992) Comparative binding of etretinate and acitretin to plasma proteins and erythrocytes. *Biochem Pharm* **44:** 1891–1893.

Wang C, Cao B, Liu Q-Q, Zou Z-Q, Liang Z-A, Gu L, Dong J-P, Liang L-R, Li W-X, Hu K, He X-S, Sun Y-H, An Y, Yang T, Cao Z-X, Guo Y-M, Wen X-M, Wang Y-G, Liu Y-L, and Jiang L-D (2011) Oseltamivir compared with the Chinese traditional therapy Maxingshigan–Yinqiaosan in the treatment of H1N1 influenza. *Ann Intern Med* **155:** 217–225.

Williams AJ, Ekins S, Spjuth O, and Willighagen EL (2012) Accessing, using, and creating chemical property databases for computational toxicology modeling. *Methods Mol Biol* **929:** 221–241.

Yin Q and Li C-S (2014) Treatment effects of XueBiJing injection in severe septic patients with disseminated intravascular coagulation. *Evid Based Complement Alternat Med* **2014:** 949254.

Zhang B-L and Chen C-H (2016) *Mordernization of Chinese Medicine for Twenty Years: 1996–2015*. Shanghai Science & Technology Press, Shanghai.

Zhang L, Li P, Xing C-Y, Zhao J-Y, He Y-N, Wang J-Q, Wu X-F, Liu Z-S, Zhang A-P, Lin H-L, Ding X-Q, Yin A-P, Yuan F-H, Fu P, Hao L,Miao L-N, Xie R-J, Wang R, Zhou C-H, Guan G-J, Hu Z, Lin S, Chang M, Zhang M, He L-Q, Mei C-L, Wang L, and Chen X-M (2014) Efficacy and safety of *Abelmoschus manihot* for primary glomerular disease: a prospective, multicenter randomized controlled clinical trial. *Am J Kidney Dis* **64:** 57–65.

DMD Fast Forward. Published on March 9, 2018 as DOI: 10.1124/dmd.117.079673
This article has not been copyedited and formatted. The final version may differ from this version.

Footnotes

This work was supported by the National Science & Technology Major Project of China 'Key New Drug Creation and Manufacturing Program' [Grants 2009ZX09304-002, 2011ZX09201-201-23, 2017ZX09301012006]; the National Science Foundation of China for Distinguished Young Scholars [Grant 30925044]; the National Basic Research Program of China [Grant 2012CB518403]; the National Natural Science Foundation of China [Grant 81503345]; and the Strategic Priority Research Program of the Chinese Academy of Sciences [Grant XDA12050306].

This work was presented in part as a poster presentation at the CPSA, Shanghai, China, April 15–18, 2015: Zhang N-T et al. Systemic exposure to and disposition of phthalides from *Ligusticum chuanxiong* rhizomes and *Angelica sinensis* roots after intravenous administration of XueBiJing injection in human subjects and rats.

Professor Chuan Li is the person to receive reprint requests with the address of 501 Haike Road, Shanghai 201203, China, and the email address of chli@simm.ac.cn.

[1]Sun Yan: current address, Laboratory of Phase I Clinical Trials, Fudan University Shanghai Cancer Center, Shanghai 200032, China.

[2]Qi Wen: visiting postgraduate student from Hainan Medical University, Hainan, China.

DMD Fast Forward. Published on March 9, 2018 as DOI: 10.1124/dmd.117.079673
This article has not been copyedited and formatted. The final version may differ from this version.

Figure Legends

Fig. 1. Phthalides detected in XueBiJing. (A) Stacked chromatogram of phthalides, detected by mass spectrometry, in XueBiJing. (B) and (C) Stacked chromatograms of phthalides, detected by mass spectrometry, in XueBiJing's component herbs Chuanxiong (*L. chuanxiong* rhizomes) and Danggui (*A. sinensis* roots), respectively. (D) Mean doses of phthalides from nine lots of XueBiJing at 100 ml/day. (E) Percentage daily doses of phthalides in the total daily dose of phthalides from XueBiJing. See Table 1 for the compounds' names.

Fig. 2. Circulating phthalides, in human subjects (n = 12) and rats (n = 6) that intravenously received XueBiJing, and their chemical structures. Human plasma (A) and urine data (B): XueBiJing, 1.25-h infusion at 100 ml/subject. Rat plasma (C), urine (D), and bile data (E): XueBiJing, 0.5-h infusion at 10 ml/kg. (A)–(E) XueBiJing phthalides (shown as compound ID) are ranked in the same order as they are ranked in Fig. 1D (mean doses of phthalides from nine lots of XueBiJing at 100 ml/day). $AUC_{0-\infty}$, area under concentration-time curve from 0 to infinity; $Cum.A_{e\text{-}U\ 0-24h}$, cumulative amount excreted into urine from 0 to 24 h; $Cum.A_{e\text{-}B\ 0-24h}$, cumulative amount excreted into bile from 0 to 24 h.

Fig. 3. High selectivity of senkyunolide I for human UGT2B15. (A) Glucuronidation activities of cDNA-expressed human UGT isoforms on senkyunolide I (50 μM). Senkyunolide I-7-*O*-β-glucuronide (**M15$_{G-2}$**) was preferentially formed, while senkyunolide I-6-*O*-β-glucuronide (**M15$_{G-1}$**) was a minor metabolite. (B) Comparative metabolic capabilities of human UGT1A9, UGT2B15, and UGT2B17 in mediating the glucuronidation of senkyunolide I into **M15$_{G-2}$**.

Fig. 4. Dehydrated GSH conjugates of senkyunolide I (**M15$_{GSH-1}$** and **M15$_{GSH-2}$**) formed in vitro by GSH replacement of glucuronic acid in a second metabolic reaction. (A) Experiments of in vitro glucuronidation and GSH conjugation of senkyunolide I. (B) Detection of metabolites of senkyunolide I and their relative abundance. UGT, uridine 5′-diphosphoglucuronosyltransferase; RLM, rat liver microsomes; HLM, human liver microsomes.

Fig. 5. Proposed metabolic pathways of senkyunolides I (**15**; A) and G (**12**; B) from intravenously dosed XueBiJing. UGT, uridine 5′-diphosphoglucuronosyltransferase; UDP, uridine 5′-diphosphate; Glu, glucuronosyl; γ-GT, γ-glutamyl transpeptidase. Metabolite ID provides information regarding parent compound, metabolite type, and metabolite isomer. For instance, M15 in **M15$_{G-1}$** denotes that the compound is a metabolite of senkyunolide I (**15**). The subscript letter G denotes glucuronide and the subscript number 1 denotes the first eluted metabolite isomer. The subscript letters GSH, Cys-Gly, and Cys denote dehydrated glutathione conjugate, cysteinylglycine conjugate, and cysteine conjugate, respectively. **M12$_{G}$** indicates only one senkyunolide G glucuronide detected.

Fig. 6. Mean plasma concentrations of senkyunolides I (**15**; A–C) and G (**12**; D–F) over time in human subjects. (A) and (D): day 1 data of human subjects who received a 1.25-h intravenous infusion of 100-ml XueBiJing (n = 12), a 2.5-h infusion of 100-ml XueBiJing (n = 12), or a 1.25-h infusion of 50-ml XueBiJing (n = 12). (B) and (E): day 7 data of the six male subjects who received a 1.25-h intravenous infusion of 50-ml preparation of XueBiJing each day for seven consecutive days. (C) and

DMD Fast Forward. Published on March 9, 2018 as DOI: 10.1124/dmd.117.079673
This article has not been copyedited and formatted. The final version may differ from this version.

(F): daily maximum plasma concentration in human subjects who received a 1.25-h intravenous infusion of 50-ml preparation of XueBiJing each day for seven consecutive days (n = 6).

Fig. 7. Mean plasma concentrations and tissue exposure levels over time of senkyunolide I (**15**) in rats that received XueBiJing or an injectable solution of purified senkyunolide I. (A) Rats received a 0.5-h intravenous infusion of XueBiJing at 10, 30, or 90 ml/kg (n = 6). (B) Rats received a 0.5-h intravenous infusion of XueBiJing at 10 ml/kg (each milliliter of XueBiJing containing 0.3 μmol of **15**) or an injectable solution of purified senkyunolide I at 3.0 μmol/kg (n = 6). (C) Tissue and systemic exposure to unchanged **15** in rats that received an intravenous bolus dose of XueBiJing at 10 ml/kg (n = 5, for each time point). AUC-based partition coefficients (K_P) of unchanged **15** between tissues and plasma were 1.10, 1.39, 1.80, 2.39, and 0.99 for the lungs, heart, brain, kidneys, and liver, respectively.

TABLE 1

Phthalides detected in samples of nine lots of XueBiJing

The nine lots of samples of XueBiJing were 1309271, 1309281, 1309291, 1309301, 1405301, 1406161, 1408191, 1410081, and 1501181. The details of detection, characterization, and quantification of phthalides in XueBiJing are described in *Supplemental Materials and Methods* (Detection and Characterization of Unchanged and Metabolized Phthalides and Quantification of Phthalides). The dose level data represent mean ± S.D. for samples of nine lots of XueBiJing.

ID	Compound	LC/TOF-MS^E Data			Molecular Mass	Molecular Formula	Log*P*	Dose Level	Lot-to-Lot Variability (RSD)
		t_R	Sodiated Molecule	Collision-Induced Fragmentation Profile					
		min	*m/z*	*m/z*	*Da*			*μmol/day*	*%*
15	Senkyunolide I	14.07	247.0946	207.1021[a], 189.0919, 161.0968	224.1049	$C_{12}H_{16}O_4$	0.8	29.31 ± 2.81	9.6
16	Senkyunolide H	14.61	247.0944	207.1019[a], 189.0916, 161.0968	224.1049	$C_{12}H_{16}O_4$	0.8	6.48 ± 0.63	9.7
12	Senkyunolide G	18.44	231.1005	191.1072[a], 149.0610, 135.0445	208.1099	$C_{12}H_{16}O_3$	1.5	4.45 ± 0.31	6.9
17	Senkyunolide N	12.36	249.1111	191.1064, 163.1116, 149.0602[a]	226.1205	$C_{12}H_{18}O_4$	1.2	4.08 ± 0.52	12.7
10	3-Hydroxy-3-*n*-butylphthalide	18.06	229.0846	189.0920, 171.0814, 133.0295[a]	206.0943	$C_{12}H_{14}O_3$	2.3	3.76 ± 0.48	12.6
9	*Z*-6,7-Epoxyligustilide	16.30	229.0840	189.0907[a], 161.0972, 143.0867	206.0943	$C_{12}H_{14}O_3$	1.7	1.27 ± 0.05	4.0
14	6,7-Dihydroxyligustilide	13.24	247.0939	207.1029, 189.0916, 161.0972[a]	224.1049	$C_{12}H_{16}O_4$	0.8	1.09 ± 0.11	10.2
6	Senkyunolide A	19.53	215.1053	193.1233[a], 175.1128, 147.1178	192.1150	$C_{12}H_{16}O_2$	3.0	0.48 ± 0.26	54.0
18	Senkyunolide J	13.27	249.1094	191.1069, 163.1124, 153.0554[a]	226.1205	$C_{12}H_{18}O_4$	1.2	0.34 ± 0.04	12.7
11	4-Hydroxy-3-*n*-butylphthalide	18.72	229.0835	161.0972, 151.0392[a]	206.0943	$C_{12}H_{14}O_3$	2.7	0.24 ± 0.03	12.6

LC/TOF-MS, liquid chromatography/time-of-flight mass spectrometry; t_R, retention time; Log*P*, octanol-water partition coefficient; RSD, relative standard deviation.
[a]Product ion of base peak.

TABLE 2

In vitro metabolism of senkyunolides I and G

The details of in vitro metabolism studies of senkyunolides I and G are described in *Supplemental Materials and Methods* (Metabolism Studies).

Subcellular Fraction	Cofactor	Metabolite ID[a]	LC/TOF-MS^E Data			Molecular Mass	Molecular Formula	Presence in In Vivo Sample
			t_R	Ionized Molecule	Diagnostic FI or NL			
			min	*m/z*	*m/z or Da*	*Da*		
Substrate: senkyunolide I								
Rat liver microsomes	UDP-GlcUA	**M15$_{G-1}$**	12.71	$[M+Na]^+$/423.1259	NL, 176.0317	400.1369	$C_{18}H_{24}O_{10}$	Rat bile and urine
		M15$_{G-2}$	13.40	$[M+Na]^+$/423.1268	NL, 176.0321			Rat bile and urine
	UDP-GlcUA + GSH	**M15$_{G-1}$**	12.73	$[M+Na]^+$/423.1266	NL, 176.0323			Rat bile and urine
		M15$_{G-2}$	13.40	$[M+Na]^+$/423.1266	NL, 176.0323			Rat bile and urine
		M15$_{GSH-1}$	14.70	$[M+H]^+$/514.1844	NL, 129.0425	513.1781	$C_{22}H_{31}N_3O_9S$	Rat bile
				$[M-H]^-$/512.1703	FI, 272.0886			
		M15$_{GSH-2}$	15.67	$[M+H]^+$/514.1857	NL, 129.0428			Rat bile
				$[M-H]^-$/512.1702	FI, 272.0882			
Human liver microsomes	UDP-GlcUA	**M15$_{G-1}$**	12.72	$[M+Na]^+$/423.1264	NL, 176.0318	400.1369	$C_{18}H_{24}O_{10}$	Human urine
		M15$_{G-2}$	13.38	$[M+Na]^+$/423.1267	NL, 176.0321			Human urine
	UDP-GlcUA + GSH	**M15$_{G-1}$**	12.72	$[M+Na]^+$/423.1252	NL, 176.0323			Human urine
		M15$_{G-2}$	13.40	$[M+Na]^+$/423.1268	NL, 176.0324			Human urine
		M15$_{GSH-1}$	14.71	$[M+H]^+$/514.1846	NL, 129.0422	513.1781	$C_{22}H_{31}N_3O_9S$	N.D. in human samples
				$[M-H]^-$/512.1700	FI, 272.0883			
		M15$_{GSH-2}$	15.67	$[M+H]^+$/514.1860	NL, 129.0428			N.D. in human samples
				$[M-H]^-$/512.1703	FI, 272.0883			
Substrate: senkyunolide G								
Rat liver microsomes	UDP-GlcUA	**M12$_G$**	16.63	$[M+Na]^+$/407.1319	NL, 176.0319	384.1420	$C_{18}H_{24}O_9$	Rat bile and urine

LC/TOF-MS, liquid chromatography/time-of-flight mass spectrometry; t_R, retention time; FI, fragment ion; NL, neutral loss; N.D., not detected.

[a]Metabolite ID provides information regarding parent compound, metabolite type, and metabolite isomer. For instance, M15 in **M15$_{G-1}$** denotes that the compound is a metabolite of senkyunolide I (**15**). The subscript letter G denotes glucuronide and the subscript number 1 denotes the first eluted metabolite isomer. The subscript letter GSH denotes dehydrated glutathione conjugate. **M12$_G$** indicates only one senkyunolide G glucuronide detected.

TABLE 3

Pharmacokinetics of senkyunolides I (**15**) and G (**12**) in human subjects who received an intravenous infusion of XueBiJing

The details of human pharmacokinetic study are described in *Supplemental Materials and Methods* (Human Pharmacokinetic Study of XueBiJing). Senkyunolide G (**12**) was not detected in human urine after dosing XueBiJing. The data represent mean ± S.D. For both phthalides, no significant gender differences in maximum plasma concentration (C_{max}), area under concentration-time curve from 0 to infinity ($AUC_{0-\infty}$), apparent volume of distribution at steady state (V_{SS}), and total plasma clearance ($CL_{tot,p}$) were observed after dose correction with the subject's body weight (P = 0.13–0.99).

Pharmacokinetic Parameter	Dosage Regimen 1 (1.25-h infusion, 100 ml/day)		Dosage Regimen 2 (2.5-h infusion, 100 ml/day)		Dosage Regimen 3 (1.25-h infusion, 50 ml/day)	
	Male (n = 6)	Female (n = 6)	Male (n = 6)	Female (n = 6)	Male (n = 6)	Female (n = 6)
*Senkyunolide I (**15**)*						
C_{max} (nM)	313 ±57 (at 1.25 h after starting the infusion, but before terminating the infusion)	391 ±63	262 ±31 (at 2.5 h after starting the infusion, but before terminating the infusion)	328 ±31	165 ±23 (at 1.25 h after starting the infusion, but before terminating the infusion)	212 ±32
$AUC_{0-\infty}$ (nM·h)	571 ±115	690 ±144	713 ±84	863 ±97	280 ±23	374 ±66
$t_{1/2}$ (h)	0.87 ±0.09	0.79 ±0.12	0.87 ±0.25	0.98 ±0.13	0.68 ±0.14	0.79 ±0.11
MRT (h)	1.73 ±0.14	1.69 ±0.21	2.41 ±0.25	2.65 ±0.19	1.52 ±0.19	1.79 ±0.23
V_{SS} (l/kg)	1.28 ±0.10	1.24 ±0.14	1.45 ±0.15	1.59 ±0.09	1.13 ±0.13	1.22 ±0.23
$CL_{tot,p}$ (l/h/kg)	0.748 ±0.096	0.746 ±0.130	0.610 ±0.116	0.605 ±0.071	0.745 ±0.064	0.683 ±0.087
CL_R (l/h/kg)	0.030 ±0.002	0.039 ±0.014	0.025 ±0.011	0.029 ±0.007	0.021 ±0.008	0.025 ±0.004
$f_{e\text{-}U}$ (%)	4.13 ±0.61	5.14 ±1.28	4.27 ±1.91	4.76 ±0.73	3.71 ±1.23	4.70 ±1.16
$CL_R/(GFR \times f_u)$ ratio	0.51 ±0.03	0.65 ±0.23	0.42 ±0.17	0.49 ±0.11	0.35 ±0.12	0.43±0.06
*Senkyunolide G (**12**)*						
C_{max} (nM)	424 ±44 (at 1.25 h after starting the infusion, but before terminating the infusion)	498 ±98	379 ±41 (at 2.5 h after starting the infusion, but before terminating the infusion)	437 ±78	238 ±52 (at 1.25 h after starting the infusion, but before terminating the infusion)	302 ±45
$AUC_{0-\infty}$ (nM·h)	1503 ±176	1799 ±333	1622 ±229	1978 ±258	779 ±284	1105 ±209
$t_{1/2}$ (h)	2.18 ±0.27	2.45 ±0.42	2.31 ±0.35	2.26 ±0.45	1.91 ±0.41	2.20 ±0.51
MRT (h)	3.72 ±0.32	4.08 ±0.56	4.52 ±0.52	4.54 ±0.58	3.33 ±0.52	3.79 ±0.74
V_{SS} (l/kg)	0.10 ±0.01	0.11 ±0.01	0.12 ±0.01	0.12 ±0.01	0.09 ±0.01	0.08 ±0.01
$CL_{tot,p}$ (l/h/kg)	0.027 ±0.002	0.028 ±0.004	0.026 ±0.005	0.026 ±0.004	0.028 ±0.007	0.023 ±0.004

MRT, mean residence time; CL_R, renal clearance; $f_{e\text{-}U}$, fractional urinary excretion; GFR, glomerular filtration rate; f_u, unbound fraction of compound in plasma.

TABLE 4

Plasma pharmacokinetics of senkyunolide I (**15**) in rats that received a 0.5-h intravenous infusion of XueBiJing at 10, 30, or 90 ml/kg and summarized results from dose proportionality assessment

The details of the rat pharmacokinetic study are described in *Supplemental Materials and Methods* (Supportive Rat Pharmacokinetic Studies of XueBiJing). The data represent mean ± S.D. Correlation was statistically significant with $P < 0.05$. Critical interval was 0.90–1.10 for the plasma pharmacokinetic data of **15**. The term "linear" was concluded statistically if the 90% confidence interval (90% CI) for slope was contained completely within the critical interval; "inconclusive" was concluded statistically if the 90% CI lay partly within the critical interval; "nonlinear" was concluded statistically if the 90% CI was entirely outside the critical interval.

Pharmacokinetic Parameter	Assessment of Plasma Pharmacokinetics			Assessment of Dose Proportionality			
	10 ml/kg (n = 6)	30 ml/kg (n = 6)	90 ml/kg (n = 6)	r	P	Slope (90% CI)	Conclusion
C_{max} (nM)	990 ± 106	2722 ± 262	8838 ± 536	0.99	1.8×10^{-17}	1.00 (0.95–1.04)	Linear
$AUC_{0-\infty}$ (nM·h)	574 ± 71	1628 ± 135	5560 ± 499	0.99	5.2×10^{-17}	0.99 (0.99–1.08)	Linear
$t_{1/2}$ (h)	0.19 ± 0.03	0.21 ± 0.01	0.24 ± 0.02	—	—	—	—
MRT (h)	0.45 ± 0.03	0.48 ± 0.02	0.53 ± 0.02	—	—	—	—
V_{SS} (l/kg)	2.19 ± 0.11	2.39 ± 0.15	2.28 ± 0.15	—	—	—	—
$CL_{tot,p}$ (l/h/kg)	4.853 ± 0.545	5.019 ± 0.411	4.396 ± 0.417	—	—	—	—

C_{max}, maximum plasma concentration; $AUC_{0-\infty}$, area under concentration-time curve from 0 to infinity; MRT, mean residence time; V_{SS}, apparent volume of distribution at steady state; $CL_{tot,p}$, total plasma clearance.

TABLE 5

Pharmacokinetic data related to in vivo reach of circulating XueBiJing phthalides

The details of in vitro pharmacokinetic studies are described in *Supplemental Materials and Methods* (Supportive In Vitro Characterizations of Phthalides). The quoted volumes of total body water, intracellular fluids, extracellular fluids, and plasma for a 70 kg man are 0.60, 0.34, 0.26, and 0.04 l/kg, respectively, whereas such volumes for a 0.25 kg rat are 0.67, 0.37, 0.30, and 0.03 l/kg, respectively (Davies and Morris, 1993). XueBiJing compounds with volume of distribution at steady state (V_{SS}) in human larger than 0.26 l/kg are predicted to have intracellular reach. Membrane permeability was determined based on apparent permeability coefficient (P_{app}) value of the compound measured on Caco-2 cell monolayers, with a P_{app} value < 0.2×10^{-6}, 0.2×10^{-6}–2.8×10^{-6}, and > 2.8×10^{-6} cm/s indicating low, intermediate, and high membrane permeability, respectively (Li et al., 2012).

Compound	V_{SS}		Detection in Rat Brain	f_u		Membrane Permeability, Caco-2 Cell-based P_{app} (EfR)	B/P Ratio	
	Human	Rat		Human	Rat		Human	Rat
	l/kg	*l/kg*		*%*	*%*			
Senkyunolide I (**15**)	1.18 ± 0.17	2.19 ± 0.11	Detected; K_P, 1.8	53.6	48.3	Good, 39.0×10^{-6} (1.2)	0.69	0.82
Senkyunolide G (**12**)	0.09 ± 0.01	0.85 ± 0.10	Not detected	3.0	13.3	Good, 27.8×10^{-6} (1.4)	0.62	0.61
Senkyunolide H (**16**)	1.19 ± 0.12	2.02 ± 0.06	Detected; K_P, 1.0	49.8	48.1	Good, 34.7×10^{-6} (1.3)	N.M.	0.78
Senkyunolide N (**17**)	0.98 ± 0.26	1.18 ± 0.07	Detected; K_P, 1.4	76.0	74.6	Good, 17.3×10^{-6} (1.4)	N.M.	0.90
3-Hydroxy-3-*n*-butylphthalide (**10**)	0.22 ± 0.04	0.64 ± 0.12	Not detected	17.9	18.1	Good, 3.62×10^{-6} (2.4)	N.M.	0.74

K_P, AUC-based partition coefficient of compound between brain and plasma; f_u, unbound fraction of compound in plasma; EfR, efflux ratio; B/P ratio, blood-to-plasma concentration ratio; N.M., not measured.

DMD Fast Forward. Published on March 9, 2018 as DOI: 10.1124/dmd.117.079673
This article has not been copyedited and formatted. The final version may differ from this version.

TABLE 6

Binding of senkyunolides I and G to individual proteins of human plasma and the proteins' relative binding capability

The details of the in vitro pharmacokinetic study are described in *Supplemental Materials and Methods* [Assessment of Protein Binding (Total Plasma and Individual Proteins)]. The binding percentage in isolated plasma protein solution represents mean ± S.D.

Human Plasma Protein	[P]	Binding Percentage in Isolated Plasma Protein Solution	n*K*	n*K*×[P]: Binding Capability	Relative Binding Capability[a]
	μM	*%*	*1/μM*		*%*
Senkyunolide I					
Albumin	600	40.5 ± 3.5	0.001	0.68	48.6
α_1-Acid glycoprotein	10	5.8 ± 3.2	0.009	0.09	6.4
γ-Globulins	80	8.7 ± 3.2	0.001	0.12	8.3
High density lipoproteins	10	6.6 ± 3.9	0.013	0.13	9.2
Low density lipoproteins	1	18.8 ± 4.3	0.260	0.26	18.2
Very low density lipoproteins	0.1	6.7 ± 3.6	1.300	0.13	9.3
Senkyunolide G					
Albumin	600	98.7 ± 0.4	0.095	56.7	99.0
α_1-Acid glycoprotein	10	4.7 ± 2.8	0.009	0.09	0.2
γ-Globulins	80	5.4 ± 2.3	0.001	0.05	0.1
High density lipoproteins	10	3.7 ± 2.6	0.006	0.06	0.1
Low density lipoproteins	1	8.2 ± 1.7	0.120	0.12	0.2
Very low density lipoproteins	0.1	12.1 ± 5.3	2.600	0.26	0.4

[P], reported protein concentration in human plasma under physiological conditions (Urien et al., 1992); n*K*, total binding constant.

[a]Calculated by $\{(nK_{protein} \times [protein])/(nK_{albumin} \times [albumin] + nK_{\alpha 1\text{-acid glycoprotein}} \times [\alpha_1\text{-acid glycoprotein}] + nK_{\gamma\text{-globulins}} \times [\gamma\text{-globulins}] + nK_{high\ density\ lipoproteins} \times [high\ density\ lipoproteins] + nK_{low\ density\ lipoproteins} \times [low\ density\ lipoproteins] + nK_{very\ low\ density\ lipoproteins} \times [very\ low\ density\ lipoproteins])\} \times 100\%$.

DMD Fast Forward. Published on March 9, 2018 as DOI: 10.1124/dmd.117.079673
This article has not been copyedited and formatted. The final version may differ from this version.

Figure 1

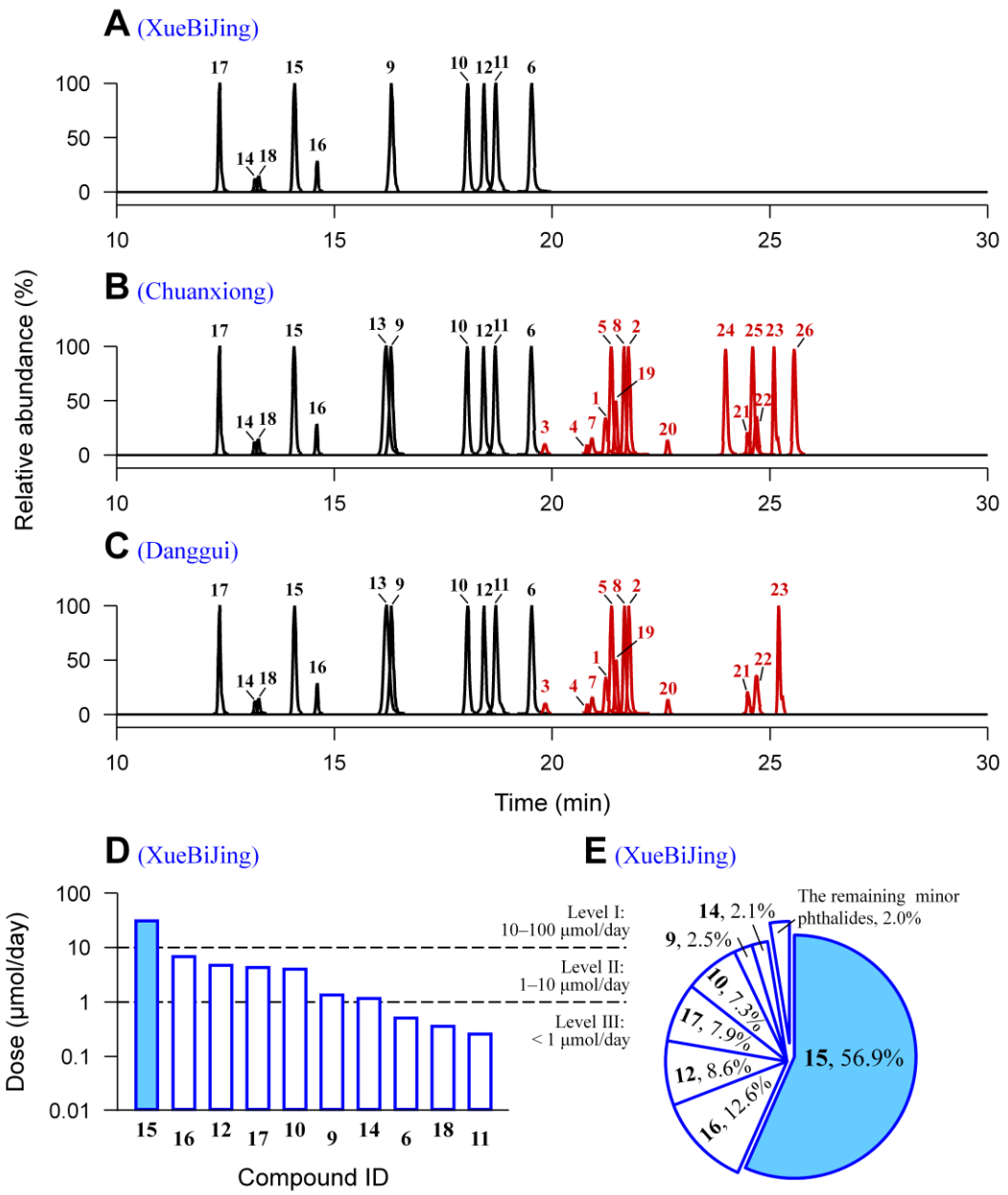

DMD Fast Forward. Published on March 9, 2018 as DOI: 10.1124/dmd.117.079673
This article has not been copyedited and formatted. The final version may differ from this version.

Figure 2

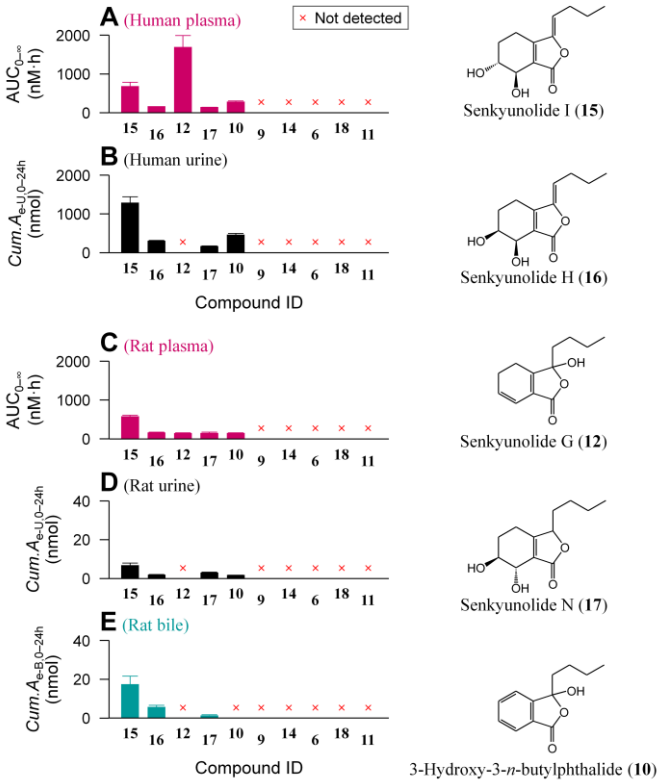

DMD Fast Forward. Published on March 9, 2018 as DOI: 10.1124/dmd.117.079673
This article has not been copyedited and formatted. The final version may differ from this version.

Figure 3

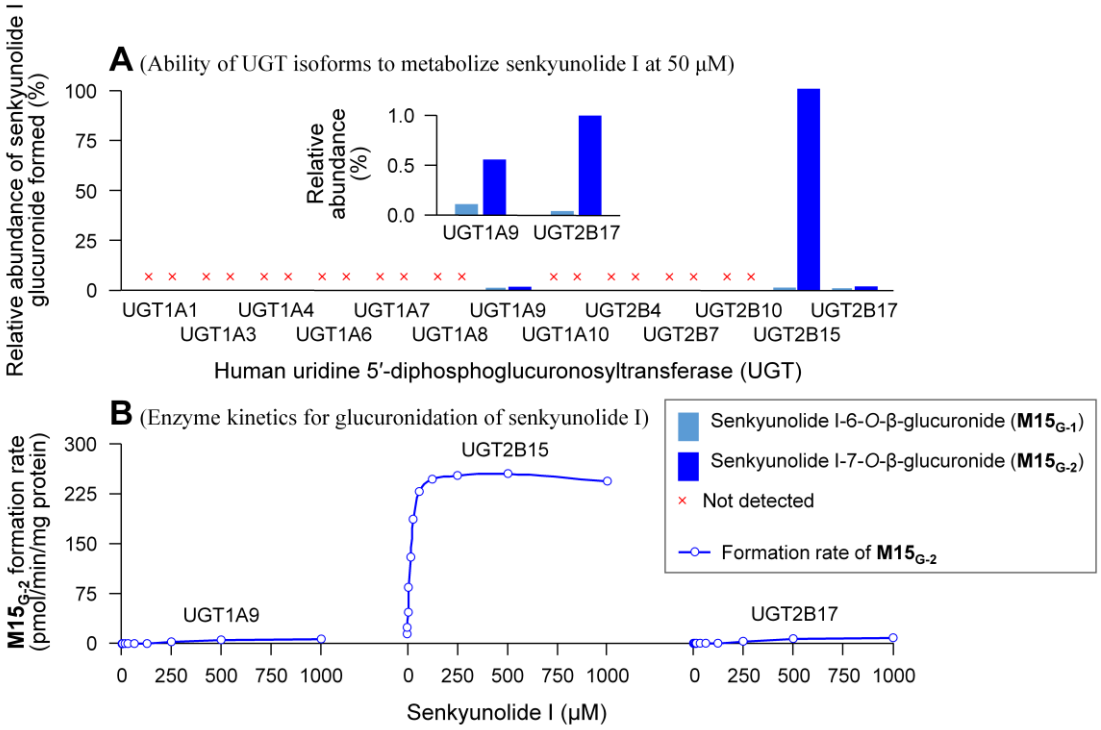

DMD Fast Forward. Published on March 9, 2018 as DOI: 10.1124/dmd.117.079673
This article has not been copyedited and formatted. The final version may differ from this version.

Figure 4

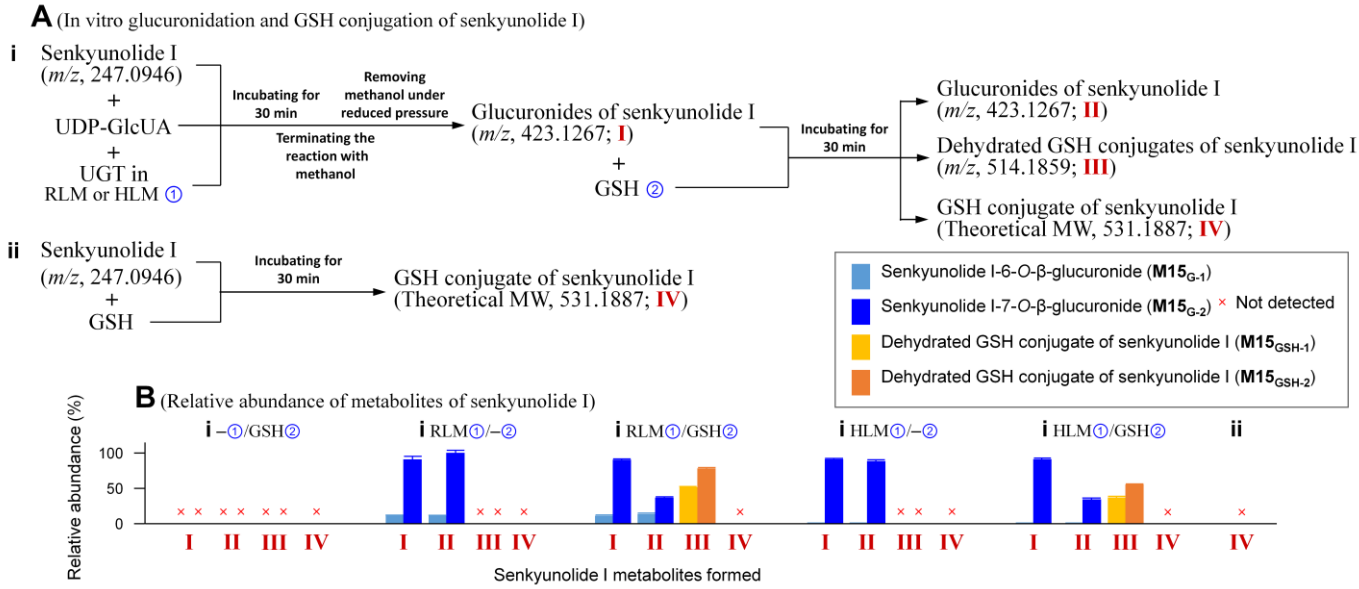

DMD Fast Forward. Published on March 9, 2018 as DOI: 10.1124/dmd.117.079673
This article has not been copyedited and formatted. The final version may differ from this version.

Figure 5

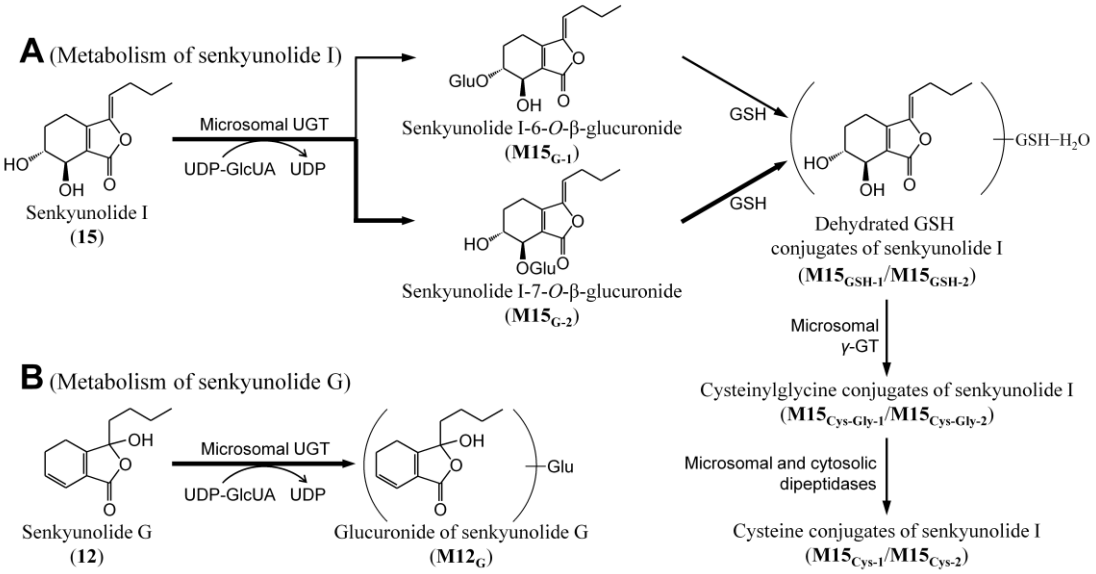

DMD Fast Forward. Published on March 9, 2018 as DOI: 10.1124/dmd.117.079673
This article has not been copyedited and formatted. The final version may differ from this version.

Figure 6

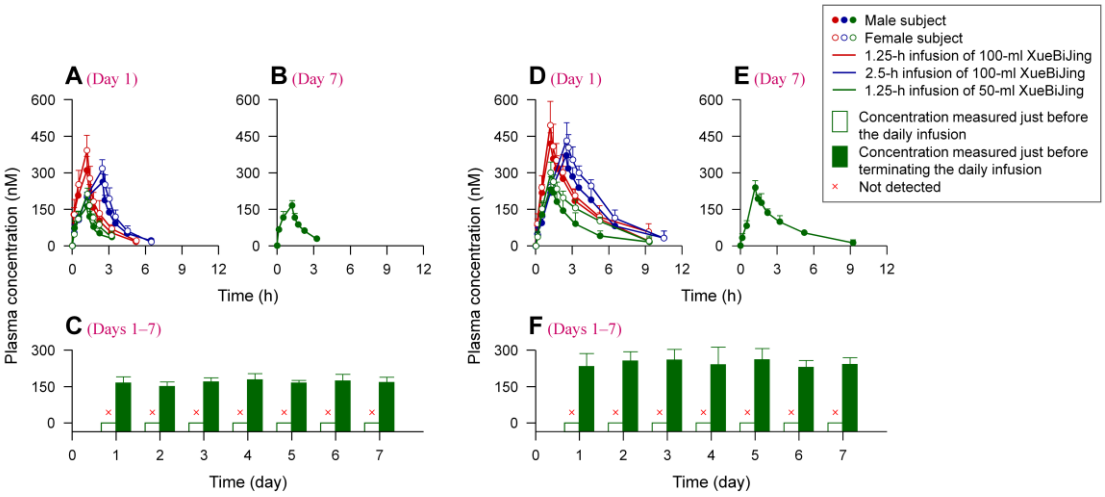

DMD Fast Forward. Published on March 9, 2018 as DOI: 10.1124/dmd.117.079673
This article has not been copyedited and formatted. The final version may differ from this version.

Figure 7